AJNR

# Regional and Global Changes in Cerebral Diffusion with Normal Aging

Annette O. Nusbaum, Cheuk Y. Tang, Monte S. Buchsbaum, Tsei Chung Wei and Scott W. Atlas

*AJNR Am J Neuroradiol* 2001, 22 (1) 136-142
http://www.ajnr.org/content/22/1/136

*AJNR Am J Neuroradiol* 22:136–142, January 2001

# Regional and Global Changes in Cerebral Diffusion with Normal Aging

Annette O. Nusbaum, Cheuk Y. Tang, Monte S. Buchsbaum, Tsei Chung Wei, and Scott W. Atlas

***BACKGROUND AND PURPOSE:*** **We used quantitative diffusion MR imaging to investigate the microstructural changes that occur in white matter during normal aging in order to identify regional changes in anisotropy and to quantify global microstructural changes by use of whole-brain diffusion histograms.**

***METHODS:*** **Full diffusion tensor MR imaging was performed in 20 healthy volunteers, 20 to 91 years old. Thirteen subjects also underwent high-resolution T1-weighted imaging, so that diffusion images could be coregistered and standardized to normal coordinates for statistical probability mapping. Relative anisotropy (RA) was calculated, as was linear regression of RA with age for each pixel; pixels with a significant correlation coefficient were displayed. For histographic analysis, the average apparent diffusion coefficient (ADC) histograms were calculated on a pixel-by-pixel basis. Subjects were divided into two equal groups by the median age (55 years) of the population and plotted for statistical comparison.**

***RESULTS:*** **Regional analysis showed statistically significant decreases in RA with increasing age in the periventricular white matter, frontal white matter, and genu and splenium of the corpus callosum, despite the absence of signal abnormalities on visual inspection of conventional images. Significant increases in RA were found in the internal capsules bilaterally. ADC histograms showed higher mean ADC and reduced peak height and skew in the older age group on group comparisons.**

***CONCLUSION:*** **Quantitative diffusion histograms correlate with normal aging and may provide a global assessment of normal age-related changes and serve as a standard for comparison with neurodegenerative diseases.**

Genetic, epigenetic, and environmental factors are all thought to affect the aging process (1). Overwhelming evidence suggests that aging is not regulated in the same programmed way as early development (2). The recent advent of diffusion tensor imaging (3, 4), a quantitative MR imaging method that reflects microstructural tissue composition, may further our understanding of the basis of cognitive changes that normally occur with aging as well as demonstrate otherwise occult alterations in cerebral structure that relate to development of dementia.

Received December 21, 1999; accepted after revision June 23, 2000.

From the Departments of Radiology (A.O.N., C.Y.T., T.C.W., S.W.A.) and Psychiatry (C.Y.T., M.S.B.), Mount Sinai School of Medicine, New York, NY; and the Department of Radiology, Stanford University, Stanford, CA (S.W.A.).

Supported in part by a supplement to AG05138 (Kenneth L. Davis, P.I.) to Dr. Buchsbaum.

Address reprint requests to Scott W. Atlas, MD, Department of Radiology, Stanford University Medical Center, S-047, 300 Pasteur Dr, Stanford, CA 94305.



Numerous anatomic studies (5–7) have documented the morphologic changes that occur in the brain in both white and gray matter with normal aging. Senescent atrophy in gray matter has been noted (5, 6); however, the long-standing belief that selective loss of neurons occurs in the neocortex (8, 9) has been challenged by recent studies showing that while atrophy is grossly detectable in the frontal and temporal lobes, there is no change in the total neuron population (10). Metabolic imaging studies have also tended to find decreases with age, also most prominently in the frontal region (11, 12). Several investigators have shown with autopsy studies (13) and by MR segmentation techniques (14) that selective atrophy of white matter, rather than gray matter, predominates in aging. This white matter atrophy is due to a decrease in myelinated fibers, which is accompanied by an increase in extracellular space (13). Capillary walls in the white matter also change with aging and become thinner, owing to loss of pericytes and thinner endothelial cytoplasm (15). In addition, focal white matter changes occur, reflecting loss of myelinated axons and gliosis (7), which correspond to patchy hyperintensities that are identifiable on convention-

al MR images. These and other studies (16, 17) suggest that age-related atrophy is more reflective of changes in the white matter than in the cortex.

In the aging population, conventional MR imaging has mainly provided gross neuroanatomic information, depicting the large-scale morphologic age-related changes of senescence (18). Volume loss in the cerebral hemisphere, enlargement of the lateral ventricles, patchy areas of abnormal signal intensity within the white matter (19) and basal ganglia, and progressive hypointensity correlating with iron deposition in the globus pallidus and putamen may be seen on T2-weighted MR images (6, 20).

Diffusion MR imaging is a quantifiable imaging method that is extremely sensitive to molecular water mobility. Since free water diffusion is restricted in highly organized tissues, like white matter (3, 4, 21, 22), diffusion MR imaging has the potential to be useful in assessing both normal development and disease states of cerebral white matter. Diffusion in normal cerebral white matter is directionally dependent (anisotropic) (21, 22), and therefore the diffusive transport of water is appropriately characterized by an effective diffusion tensor, *D* (23, 24). Diffusion tensor MR imaging is a method of mapping the degree of directionality of white matter pathways (3, 4, 23, 24) by providing a quantitative measure of directionally restricted (anisotropic) diffusion in tissues with an organized microstructure, like cerebral white matter. In a combined study using diffusion tensor MR imaging and functional imaging (25), regional white matter anisotropic changes corresponded to regional changes in function as inferred from brain metabolism assessed by fluorodeoxyglucose positron emission tomography in the same individuals, suggesting a link between changes in organization and changes in function. Therefore, diffusion tensor imaging permits the study of complex microstructural features in cerebral white matter and has the potential to elucidate the anatomic and pathoanatomic bases of information processing (ie, functional changes) within the brain (22).

Recent studies have attempted to analyze diffusion tensor anisotropy in the human brain as a function of normal brain development (26–28). Diffusion anisotropy in the white matter of neonates increases with gestational age (26, 27). Klingberg et al (28) found lower anisotropy in the frontal white matter in seven children (mean age, 10 years) than in five young adults (mean age, 27 years), and the right frontal area had higher values than the left. The data from these studies suggest that diffusional anisotropy is related to the development of myelination. Age-related decreases in diffusion anisotropy were identified in the pyramidal tract in the cerebral peduncle in another recent study (29). Our study extends this work through the human life span to assess adults aged 21 to 91 years, and adds statistical probability mapping for regional contrasts of the effects of aging.

Our purpose was to investigate microstructural changes of cerebral white matter during normal aging by quantitative diffusion imaging as a potential method of analyzing alterations in white matter circuitry subserving cognitive function. We sought to identify the regional changes in white matter relative anisotropy (RA) with normal aging and to quantify global microstructural changes in normal aging by using whole-brain apparent diffusion coefficient (ADC) histograms. We hypothesized that anisotropy would show regional changes and that quantitative ADC histograms might serve as a method to document global cerebral parenchymal changes in normal aging.

## Methods

Twenty volunteers (seven women and 13 men, 20–91 years old) established to be healthy by serum chemistries and medical history, underwent MR imaging on a 1.5-T unit modified with hardware for echo-planar imaging. Subjects represented eight decades of life with the following composition: third decade (n = 2), fourth decade (n = 6), fifth decade (n = 1), sixth decade (n = 3), seventh decade (n = 3), eighth decade (n = 2), ninth decade (n = 2), 10th decade (n = 1).

Diffusion imaging parameters were as follows: TR/TE/excitations = 10,000/99/4, TI = 220, slice thickness = 5 mm, interslice gap = 2.5 mm, FOV = 24 × 24 cm, matrix = 128 × 128, number of slices = 14. Eight images were acquired per slice, seven with a b value of 750 s/mm$^2$ and the eighth with a b value of 0 s/mm$^2$. This eighth image is equivalent to a T2-weighted image and was used for clinical screening by one of the authors. Axial T1-weighted 3D spoiled gradient-recalled (SPGR) images (600/5, FOV = 24 cm, slice thickness = 1.2 mm, flip angle = 40°, matrix = 256 × 256) were also acquired during the same scanning session. Thirteen of these same subjects (10 men and three women) also underwent high-resolution T1-weighted imaging with a 3D-SPGR sequence, so that diffusion images could be coregistered and standardized to normal coordinates for statistical probability mapping.

MR images of brains of all subjects included in this study were normal on both T1- and T2-weighted images, as determined by a neuroradiologist, with none of the subjects having more than three very small (<3 mm in diameter) areas of hyperintensity on T2-weighted images in the brain parenchyma.

The raw diffusion data were reconstructed automatically online and then transferred to an off-line workstation (Sparc 20; Sun Microsystems, Mountain View, CA) for diffusion trace calculations using software developed in IDL (Research Systems, Boulder, CO). The effective diffusion tensor, *D*, and its corresponding eigenvalues and eigenvectors were calculated for every pixel by using a program written in Matlab. The RA, defined as the magnitude of the anisotropic part of *D* divided by the magnitude of the isotropic part of *D* (3), was calculated from the diffusion tensor [$RA = \sqrt{Var(\lambda)/E(\lambda)}$] (3).

Using a standard brain atlas (30) as a reference, slices from the structural and RA images were selected and matched on the basis of visible anatomic structures. This selection resulted in seven contiguous slices that were consistently identified for all the subjects. The outlines of the brain were identified on the individual axial T1-weighted images by using software developed in-house, and midline landmark points were identified. This image morphing technique is based on a nonlinear transformation using landmarks determined by a neuroradiologist. Midline landmarks were chosen such that CSF spaces were marked by the same anchor points. This ensured that subsequent transformations would map CSF regions into CSF and tissue regions into tissue. While other image morphing algorithms that are based on global brain features or contours could

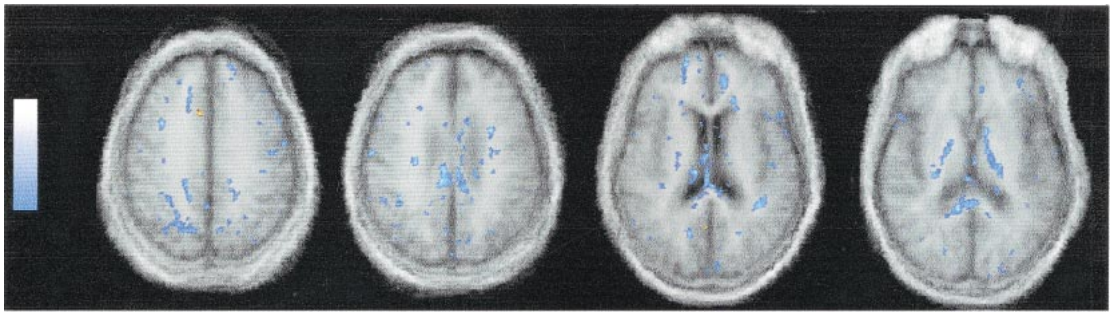

FIG 1. Statistically significant regions of decreased anisotropy with increasing age. Areas with significant anisotropic decrease with age are shown in *blue* to *blue-white* and were identified in the frontal white matter, genu and splenium of the corpus callosum, and parietal and occipital periventricular white matter. Correlation coefficients between RA and age are displayed for each pixel with the scale bar indicating the correlation coefficient from $r = -0.55$, $P < .05$ (*blue*) to the most negative correlation found, $P < .0001$ (*blue-white*). (Background is group mean, anatomically standardized, T1-weighted images at four slice locations.)

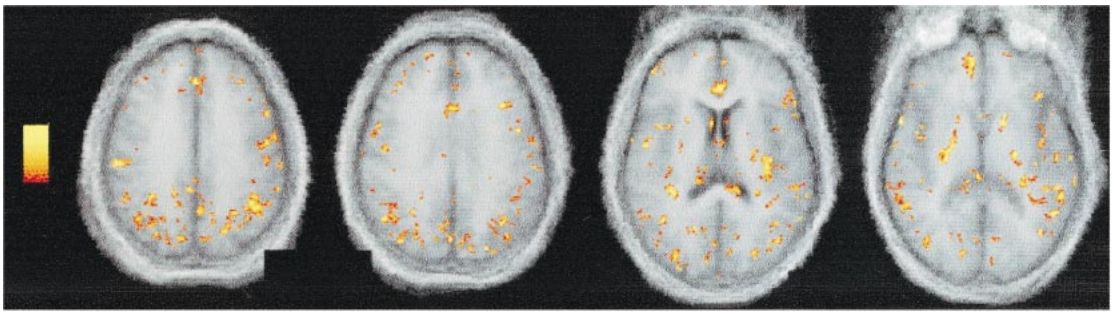

FIG 2. Statistically significant regions of increased anisotropy with increasing age. Areas of significant diffusion anisotropic increase with age are shown in *red-yellow* and were identified in the posterior limb of the internal capsules bilaterally and diffusely at the periphery of the brain, notably at the brain-CSF interfaces (most likely artifactual). Correlation coefficients are displayed using a method similar to that in Figure 1, with the correlation coefficients from $r = .55$, $P < .05$ (*red*) to the most positive correlation found, $r = .90$, $P < .0001$ (*yellow*). (Background is group mean, anatomically standardized, T1-weighted images at four slice locations.)

suffer from confounds due to age-related atrophy, significant findings near CSF-tissue interfaces should be minimized with our methodology. Each RA image was then coregistered to the matched anatomic image by using the algorithm proposed by Woods et al (31), after correction for gradient-induced distortion on diffusion images (X. Zhou, J.K. Maier, and H.G. Reynolds, ''Method to Reduce Eddy Current Effects in Diffusion-Weighted Echo Planar Imaging,'' US Patent, 5,864,233; January 26, 1999). The coregistered RA images were then standardized using the brain contour (left and right sides for every row of pixels) and nine midline anatomic landmarks to the same brain coordinate system for statistical probability mapping (32). The linear regression of diffusion anisotropy with age was calculated for each pixel, and pixels with a significant correlation coefficient were displayed (Figs 1 and 2).

The T2-weighted axial images encompassing the entire brain were then traced using a mouse-driven semiautomated software program developed in-house. Edges of the brain were obtained by tracing the brain contour from the vertex to the level of the inferior cerebellum. A separate computer program was used to apply these edges to the matching trace (average ADC) images, and all the voxel values inside the contour were extracted. A histogram was then computed for each subject with a bin-width equal to 1% of the maximum value. These histograms were then normalized across the subjects for differences in brain size (1000 pixels per whole brain) (Fig 3). The histographic peak location, peak height, skew, and brain mean ADC were obtained. Correlations between subject's age and average ADC values, peak height of ADC histograms, peak locations of ADC histograms, and skew of curves were assessed by linear regression analysis (Figs 4–7). Subjects were also divided into ''young'' and ''old'' groups as determined by their median age (55 years), and a *t* test between the young and old subjects was computed for each of the parameters. A *P* value less than .05 was considered statistically significant (Table).

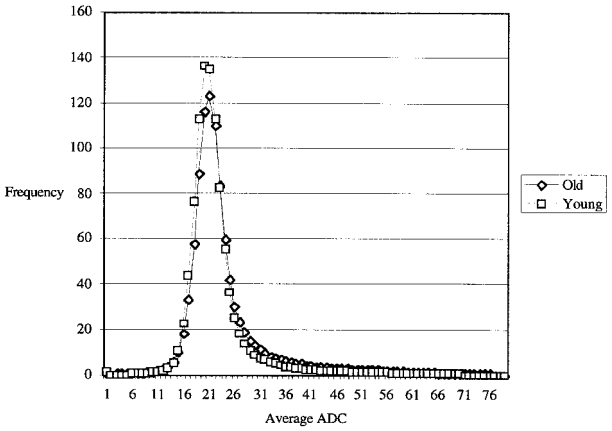


FIG 3. Averaged ADC histograms for each group of subjects (defined by age), where the *x* axis represents the average ADC values and the *y* axis scales with the number of pixels at any given ADC value.

## Results

### *Regional Anisotropy*

Statistical probability maps derived from linear regression analysis showed regional decreases in

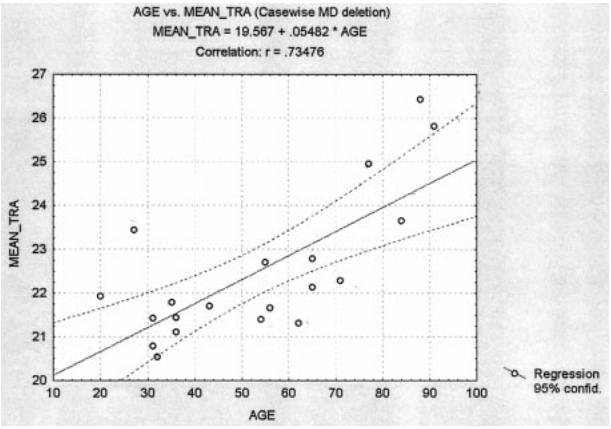


FIG 4. Average brain ADC (mean trace) versus subject's age, linear regression.

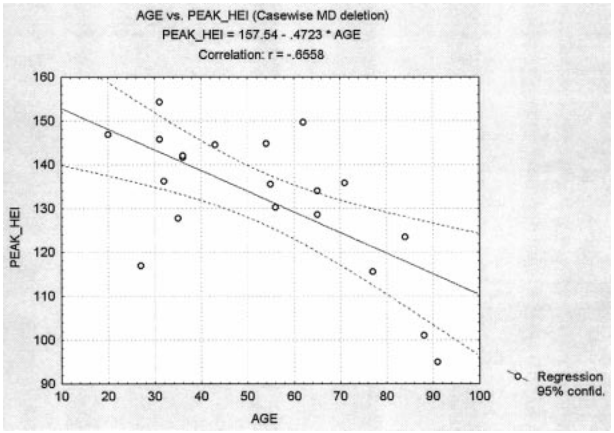


FIG 5. Peak height of ADC histogram versus subject's age, linear regression.

**Analysis of apparent diffusion coefficient histographic characteristics versus age group by *t* test**

| | % ± SD | | |
|---|---|---|---|
| | Old Subjects | Young Subjects | *P* Value |
| Peak height | 12.5 ± 1.6 | 14.0 ± 1.1 | .03 |
| Peak location ($\times 10^{-3}$ mm$^2$/s) | 20.90 ± 0.57 | 20.60 ± 0.52 | .23 (NS) |
| Brain $ADC_{ave}$ ($\times 10^{-3}$ mm$^2$/s) | 23.39 ± 1.78 | 21.56 ± 0.79 | .008 |
| Skew | 2.41 ± 0.40 | 6.82 ± 0.71 | <.0001 |

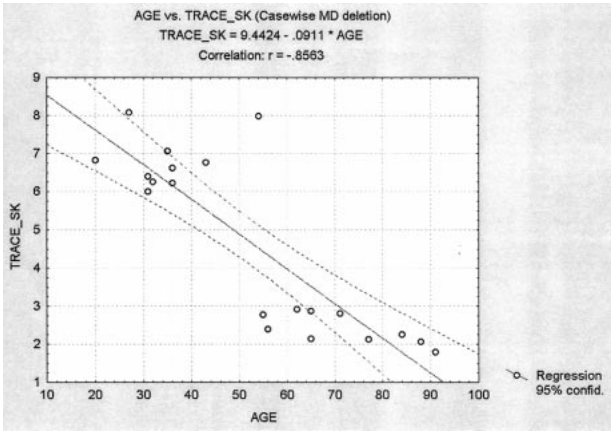


FIG 6. Skew of ADC histogram versus subject's age, linear regression.

diffusion anisotropy in frontal white matter, genu and splenium of the corpus callosum, internal capsules, and periventricular white matter with increasing age (Fig 1). Correlation coefficients with age reached statistical significance ($P < .05$) in the frontal white matter, genu and splenium of the corpus callosum, internal capsules, and parietal and occipital periventricular white matter with increasing age. Some involvement of cortical gray matter was also noted.

Increases in diffusion anisotropy were seen in the internal capsules bilaterally and diffusely at the periphery of the brain, notably at brain-CSF interfaces, with increasing age. Statistically significant ($P < .05$) increases in RA were seen in these regions (Fig 2).

### *ADC Histograms*

Average brain ADC was significantly correlated to subject's age ($r = .735$; $P = .0002$) by linear regression analysis at 95% confidence limits (Fig 4). Older subjects as a group showed higher average brain ADC relative to younger subjects ($P = .008$; *t* test) (Table). The peak height of the ADC histograms was inversely correlated to subject's age ($r = -.656$; $P = .0017$) by linear regression analysis at 95% confidence limits (Fig 5). In group comparisons, peak height of ADC histograms was significantly lower for the older group than for the younger group ($P = .026$; *t*-test) (Table). The skew of the histograms was inversely correlated to subject's age ($r = -.856$; $P < .0001$) by linear regression analysis at 95% confidence limits (Fig 6). Older subjects as a group showed lower skew of brain ADC histograms relative to younger subjects ($P < .0001$; *t* test) (Table). The peak location of the ADC histograms did not correlate with age ($r = .341$; $P = .1423$) by linear regression analysis at 95% confidence limits (Fig 7). Similarly, on group comparisons, peak ADC locations did not differ between groups ($P = .232$; *t* test) (Table).

## Discussion

Animal and human studies have long indicated that morphologic and chemical changes occur in cerebral white matter with normal aging. In aging humans, a highly significant, selective decrease in the total volume of white matter is seen at autopsy (33) and by MR imaging (14). Further studies have shown that white matter hyperintensities on MR images (7) do not clearly correspond with volume loss of white matter or with cerebral hemisphere with age (6, 14). It is also unclear whether these white matter hyperintensities on MR images cor-

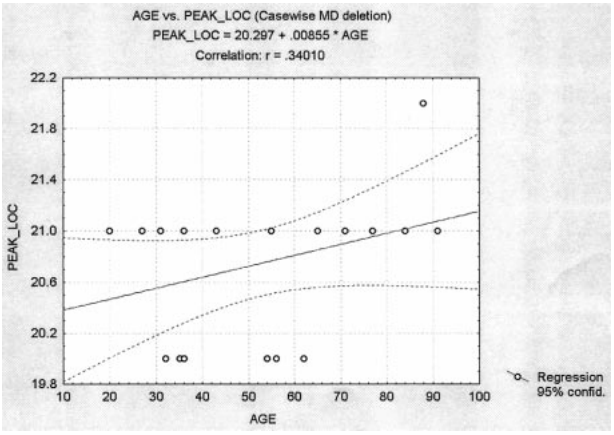


FIG 7. Peak location of ADC histogram versus subject's age, linear regression.

respond with a cognitive decline in healthy elderly subjects (34, 35). An age-related loss of cholinergic nerve fibers (36) has been reported in the cerebral cortex, suggesting that atrophy of the white matter may be due to a decrease in the number of nerve fibers. Capillary walls in the white matter also change with aging, owing to loss of pericytes and thinner endothelial cytoplasm (15), and may represent another potential cause of changes in interstitial space constituents and volume. Therefore, the preponderance of data do seem to indicate a more diffuse process in white matter that is not necessarily confined to regions of abnormal signal intensity on conventional MR images.

Our results indicate that there are both regional and global changes in brain diffusion accompanying normal aging that are present despite the absence of white matter hyperintensities. Regional data from our study point to statistically significant decreases in diffusion anisotropy in the corpus callosum, periventricular white matter, frontal white matter, internal capsules, and parietal and occipital white matter. Our data also showed some change in cortical regions. The finding of periventricular white matter anisotropic changes is intuitively in accordance with the commonly seen regional white matter signal intensity changes on conventional T2-weighted MR images in the same regions in many elderly patients (37). On histopathologic specimens, loss of myelinated axons and gliosis have been found in these same regions (7), but pathogeneses remain unclear. Since previous studies have reported diffusion MR changes despite normal brain signal intensity on conventional MR images in a variety of neuropathologic conditions (25, 38–40), we can infer that these data are further evidence of the high sensitivity of diffusion MR imaging to otherwise occult disease processes. We also note that there are potential confounds to these data, most notably the possible errors due to age-related changes in subarachnoid space volumes, so that brain-CSF interfaces might show decreases in anisotropy merely as a reflection of atrophy.

Our finding of decreased anisotropy with aging corresponds, albeit imperfectly, with the functional positron emission tomography (PET) finding of altered metabolic rates in the same subject population (11, 12). These changes, mainly in frontal regions, are postulated to reflect presumed frontal neuronal loss or alterations in cortical connectivity. Age-related changes in neural activation found on PET scans imply a more global reorganization of the networks subserving cognitive performance (11, 12). Our data are further supported by autopsy studies in humans (41) showing loss of 36% of dry brain solids, in particular myelin lipids and neuronal membranes, between the ages of 20 and 100 years. Another study (42) examined the electrophoretic protein patterns of myelin isolated from frontal and callosal white matter in patients between the ages of 17 and 90 years. These investigators found that while the proportions of the major myelin proteins remained virtually unchanged with age, the total mass of purified myelin gradually decreased with age, suggesting an age-related loss of the myelin sheath.

Our data also indicate a regional decrease in diffusion anisotropy in the genu and splenium of the corpus callosum, corroborating the findings in an autopsy study (13) in which morphometric investigation of the corpus callosum showed a loss of total nerve fiber area accompanied by an increased extracellular space with increasing age. In particular, a greater decline in the number of larger myelinated nerve fibers ($>1$ $\mu$m in diameter) than of smaller nerve fibers (0.4–0.2 $\mu$m in diameter) was found. A stereologic investigation of the white matter performed by Tang et al (33) showed that the total volume of white matter, total volume of myelinated fibers, and total length of myelinated fibers significantly decreased with age. Interestingly, this study found a greater loss of smaller-diameter myelinated fibers than of larger-diameter fibers.

Our study also defines regions of increased anisotropy with normal aging in two areas. First, some increases in anisotropy were identified diffusely at the periphery of the brain (ie, at brain-CSF interfaces). These findings were not expected and remain of uncertain origin. We caution that increases in peripheral brain-CSF interface anisotropy may be artifactual, and have been explained by Pierpaoli et al (4) as due to shearing and dilatational distortion of the diffusion-weighted images caused by eddy currents, and the misregistration of the distorted diffusion-weighted images introduces an artifact in the estimation of *D*. This results in blurring and an appearance of spurious boundaries; that is, regions of apparently increased anisotropy at the interfaces between structures that have markedly different diffusion properties. Because, with aging, the cortical sulci are deeper and CSF-brain boundaries more prominent, the cortical rim might have spuriously higher anisotropy values in older individuals. However, similar analyses of statistical probability maps on anatomic MR images from a

larger sample (11) did not show age-related changes in these areas, suggesting that sulcal widening is unlikely to contribute significantly to the findings reported here. A second area showing significant increases in anisotropy was found in the internal capsules bilaterally. The internal capsule region is not situated near any brain-CSF boundary; however, if one were to attribute this to artifacts, it may be explained by the greatly differing diffusion properties between the highly structured and ordered (anisotropic) internal capsules and the adjacent (isotropic) gray matter. Alterations in anisotropy of internal capsules could also have resulted from selective dropout of fiber bundles that could have a net result of increased or even decreased anisotropy. Errors in patient registration could also have been a confounding variable, although the peripheral change in anisotropy was not seen as an area of decreased anisotropy. Further study for confirmation and elucidation of these results is necessary.

Our data agree, in a general sense, with prior reports of diffusion MR imaging in aging, but contradict some specific aspects of those data. In a study by Gideon et al (43), significant increases in calculated ADC were found in subcortical white matter with aging. However, in that study, no ADC differences were found between various neuroanatomic regions. Moreover, corpus callosum ADC did not change with age. Numerous and significant differences in methodologies, however, can be identified between our study and that previous report. First, the previous study selected regions of interest on a single axial slice, whereas our anisotropic data examined the entire supratentorial brain. Second, our data measured RA from full tensor acquisitions, whereas the previous study measured ADC in a single diffusion direction.

The ultimate meaning and functional correlates of regional anisotropic changes in normal aging shown in this study are uncertain and will require more studies correlating neuropsychological testing and cognitive function with structural data. Prior diffusion tensor studies in schizophrenic patients showed an association between abnormalities in regional diffusion anisotropy and regional brain function, implying that diffusion anisotropy may indicate the basis of changes in cortical function (25). Therefore, our current diffusion MR data may imply changes in organization of white matter pathways that occur with normal aging that relate to altered brain function. While much of the regional changes depicted decreases in anisotropy, some areas showed an increase in anisotropy with age. This finding was unexpected and seems worthy of further study.

Our diffusion histographic data showed statistically significant differences between older and younger healthy subjects. These quantitative data have two major differences from prior diffusion data: 1) they are semiautomated, since the only operator intervention was to exclude extracranial soft tissues and calvaria from the intracranial space; and 2) they can analyze the whole brain, rather than operator-selected limited regions of interest. Our rationale for devising and using such a diffusion analysis technique is that brain aging appears at least to some extent to be a diffuse process. In fact, one notes in the literature extensive published data documenting both gray and white matter changes with aging. This method is also important because it theoretically should detect changes that occur regardless of the conventional MR appearance of the brain. Previous diffusion histographic data have been used in the setting of multiple sclerosis (44), another process that affects the brain in a diffuse manner.

For analysis of global cerebral parenchymal changes, we decided to use the diffusion trace, or average ADC, rather than diffusion anisotropy, because trace values are likely to be more sensitive to water content in general. Our data showed that for the averaged trace histogram, the peak height was significantly lower and the brain mean trace was significantly higher for the older group as compared with the younger group. An important consideration in interpreting the trace histograms is the possible confounding effect of partial volume averaging of the brain near regions that contain CSF (45, 46). Since the water in CSF has an extremely high diffusion coefficient, averaging of the brain with the CSF may result in a spurious increase in the measured trace *D* value. This effect should have been minimized in our study, since we used a fluid-attenuated inversion recovery diffusion sequence. Because the histograms are normalized for brain sizes, the peak height and the width of the histogram are inversely related. The reduced peak (wider histogram) for the elderly group is an indication of a larger spread in the trace values and may reflect heterogeneity of axonal organization in the aging group. The higher peak location and brain mean trace may be a reflection of the underlying histopathologic substrates of myelin loss, axonal fiber loss, and extracellular space increase (13, 16, 33, 41, 42, 47).

## Conclusion

Significant changes in regional anisotropy occur in the corpus callosum, internal capsules, and frontal, parietal, and occipital white matter with normal aging, despite a normal appearance on conventional MR images. Extrapolating from pathologic studies, these findings may be a reflection of the underlying ultrastructural changes found in normal aging, which include a loss of myelin and axonal fibers and an increase in extracellular space. Although much of our regional data showed decreases in anisotropy, we also found regions of increased anisotropy, an unexpected finding of uncertain significance that may be worthy of future study. Regardless of precise microstructural correlates, these diffusion MR data suggest that this technique is highly sensitive to otherwise occult disease processes and imply changes in organization of white matter pathways that occur with normal aging. Global changes in diffusion are also seen in normal

aging. Quantitative diffusion histograms may provide a global assessment of normal age-related changes and serve as a standard for comparison with neurodegenerative diseases.

## Acknowledgments

Karen Metroka, Erin Lunders, and Melissa Biren Singer provided technical support.

## References


1. Jazwinski SM. **Longevity, genes, and aging.** *Science* 1996;273: 54–58
2. Kirkwood TBL, Cremer T. **Cytogerontology since 1881: a reappraisal of August Weisman and a review of modern progress.** *Hum Genet* 1982;60:101–121
3. Basser PJ, Pierpaoli C. **Microstructural and physiological features of tissues elucidated by quantitative-diffusion-tensor MRI.** *J Magn Reson B* 1996;111:209–219
4. Pierpaoli C, Jezzard P, Basser PJ, Barnett A, Di Chiro G. **Diffusion tensor MR imaging of the human brain.** *Radiology* 1996; 201:637–648
5. Pfefferbaum A, Mathalon DH, Sullivan EV, Rawles JM, Zipursky RB, Lim KO. **A quantitative magnetic resonance imaging study of changes in brain morphology from infancy to late adulthood.** *Arch Neurol* 1994;51:874–887
6. Christiansen P, Larsson HBW, Thomsen C, Wieslander SB, Henriksson O. **Age dependent white matter lesions and brain volume changes in healthy volunteers.** *Acta Radiol* 1994;35:117–122
7. Scheltens P, Barkhof F, Leys D, Wolters EC, Ravid R, Kamphorst W. **Histopathologic correlates of white matter changes on MRI in Alzheimer's disease and normal aging.** *Neurology* 1995;45: 883–888
8. Brody H. **Organization of the cerebral cortex, III: a study of aging in the human cerebral cortex.** *J Comp Neurol* 1955;102: 551–556
9. Brody H. **Structural changes in the aging nervous system.** *Interdis Topics Gerontol* 1970;7:9–21
10. Terry RD, DeTeresa R, Hansen LA. **Neocortical cell counts in normal human adult aging.** *Ann Neurol* 1987;21:530–539
11. Hazlett EA, Buchsbaum MS, Mohs RC, et al. **Age-related shift in brain region activity during successful memory performance.** *Neurobiol Aging* 1998;19:437–445
12. Cabeza R, McIntosh AR, Tulving E, Nyberg L, Grady CL. **Age-related differences in effective neural connectivity during encoding and recall.** *Neuroreport* 1997;8:3479–3483
13. Meier-Ruge W, Ulrich J, Bruhlmann M, Meier E. **Age-related white matter atrophy in the human brain.** *Ann N Y Acad Sci* 1992;673:260–269
14. Guttman CRG, Jolesz FA, Kikinis R, et al. **White matter changes with normal aging.** *Neurology* 1998;50:972–978
15. Stewart PA, Magliocco M, Hayakawa K, et al. **A quantitative analysis of blood-brain barrier ultrastructure in the aging human.** *Microvasc Res* 1987;33:270–282
16. Meier-Ruge W, Hunziger U, Schulz U, Tobler HJ, Schweizer A. **Stereological changes in the capillary network and nerve cells of the aging human brain.** *Mech Age Dev* 1980;14:233–243
17. Takeda S, Matsuzawa T. **Age-related brain atrophy: a study with computed tomography.** *J Gerontol* 1985;40:159–163
18. Drachman DA. **Aging and the brain: a new frontier.** *Ann Neurol* 1997;42:819–828
19. Zimmerman RD, Fleming CA, Lee BC, Saint-Louis LA, Deck MD. **Periventricular hyperintensity as seen by magnetic resonance: prevalence and significance.** *AJR Am J Roentgenol* 1986; 146:443–450
20. Drayer BP. **Imaging of the aging brain, I: normal findings.** *Radiology* 1988;166:785–796
21. Moseley ME, Cohen Y, Kucharczyk J, et al. **Diffusion-weighted MR imaging of anisotropic water diffusion in cat central nervous system.** *Radiology* 1990;176:439–445
22. Basser PJ. **New histological and physiological stains derived from diffusion-tensor MR images.** *Ann N Y Acad Sci* 1997;820: 123–138
23. Stejskal EO, Tanner JE. **Spin diffusion measurements: spin echoes in the presence of time-dependent field gradient.** *J Chem Phys* 1965;42:288–292
24. Stejskal EO. **Use of spin echoes in a pulsed magnetic-field gradient to study restricted diffusion and flow.** *J Chem Phys* 1965; 43:3597–3603
25. Buchsbaum MS, Tang CY, Peled S, et al. **MRI white matter diffusion anisotropy and PET metabolic rate in schizophrenia.** *Neuroreport* 1998;9:425–430
26. Neil JJ, Shiran SI, McKinstry RC, et al. **Normal brain in human newborns: apparent diffusion coefficient and diffusion anisotropy measured by using diffusion tensor MR imaging.** *Radiology* 1998;209:57–66
27. Huppi PA, Maier SE, Peled S, et al. **Microstructural development of human newborn cerebral white matter assessed in vivo by diffusion tensor magnetic resonance imaging.** *Pediatr Res* 1998;44:584–590
28. Klingberg T, Vaidya CJ, Gabrieli JD, Moseley ME, Hedehus M. **Myelination and organization of the frontal white matter in children: a diffusion tensor MRI study.** *Neuroreport* 1999;10: 2817–2821
29. Virta A, Barnett A, Pierpaoli C. **Visualizing and characterizing white matter fiber structure and architecture in the human pyramidal tract using diffusion tensor MRI.** *Magn Reson Imaging* 1999;17:1121–1133
30. Matsui T andHirano A. ***An Atlas of the Human Brain for Computerized Tomography.*** Tokyo: Igaku-Shoin; 1978
31. Woods RP, Cherry SR, Mazziotta JC. **Rapid automated algorithm for aligning and reslicing PET images.** *J Comput Assist Tomogr* 1992;16:620–633
32. Buchsbaum MS, Hazlett EA, Haznedar MM, Spiegel-Cohen J, Wei TC. **Visualizing fronto-striatal circuitry and neuroleptic effects in schizophrenia.** *Acta Psychiatry Scand* 1999; 395(Suppl):129–137
33. Tang Y, Nyengaard JR, Pakkenberg B, Gundersen HJG. **Age-induced white matter changes in the human brain: a stereological investigation.** *Neurobiol Aging* 1997;18:609–615
34. Boone KB, Mileer BL, Lesser JM, et al. **Neuropsychological correlates of white-matter lesions in healthy elderly subjects: a threshold effect.** *Arch Neurol* 1992;49:549–554
35. Coffey CE, Figiel GS, Djang WT, Saunders WB, Weiner RD. **White matter hyperintensity on magnetic resonance imaging: clinical and neuroanatomic correlates in the depressed elderly.** *J Neuropsychiatry Clin Neurosci* 1989;1:135–144
36. Geula C, Mesulam MM. **Cortical cholinergic fibers in aging and Alzheimer's disease: a morphometric study.** *Neuroscience* 1989;33:469–481
37. Awad IA, Spetzler RF, Hodak JA, Awad CA, Carey R. **Incidental subcortical lesions identified on magnetic resonance imaging in the elderly, I: correlation with age and cerebrovascular risk factors.** *Stroke* 1986;17:1084–1089
38. Horsfield MA, Lai M, Webb SL, et al. **Apparent diffusion coefficients in benign and secondary progressive multiple sclerosis by nuclear magnetic resonance.** *Magn Reson Med* 1996; 36:393–400
39. Singer MB, Chong J, Lu D, Schonewille WJ, Tuhrim W, Atlas SW. **Diffusion-weighted MRI in acute subcortical infarction.** *Stroke* 1998;29:133–136
40. Gonzalez RG, Schaefer PW, Buonanno FS, et al. **Diffusion-weighted MR imaging: diagnostic accuracy in patients imaged within 6 hours of stroke symptom onset.** *Radiology* 1999;210:155–162
41. Svennerholm L, Bostrom K, Jungbjer B. **Changes in weight and compositions of major membrane components of human brain during the span of adult human life of Swedes.** *Acta Neuropathol* 1997;94:345–352
42. Berlet HH, Volk B. **Studies of human myelin proteins during old age.** *Mech Aging Dev* 1980;14:211–222
43. Gideon P, Thomsen C, Henriksen O. **Increased self-diffusion of brain water in normal aging.** *J Magn Reson Imaging* 1994;4: 185–188
44. Nusbaum AO, Tang CY, Wei TC, Buchsbaum MS, Atlas SW. **Whole-brain diffusion MR histograms differ between MS subtypes.** *Neurology* 2000;54:1421–1427
45. Kwong KK, McKinstry RC, Chien D, Crawley AP, Pealman JD, Rosen BR. **CSF-suppressed quantitative single-shot diffusion imaging.** *Magn Reson Med* 1991;21:157–163
46. Falconer JC, Narayana PA. **Cerebrospinal fluid-suppressed high-resolution diffusion imaging of human brain.** *J Magn Reson* 1997;37:119–123
47. Scarpelli M, Salvolini U, Diamanti L, Montironi R, Chiaromoni L, Maricotti M. **MRI and pathological examination of postmortem brains: the problem of white matter high signal areas.** *Neuroradiology* 1994;36:393–398